Research Square

Preprints are preliminary reports that have not undergone peer review.
They should not be considered conclusive, used to inform clinical practice,
or referenced by the media as validated information.

CT-based three-dimensional planning and early postoperative posterior-facet displacement after percutaneous calcaneal fixation: a retrospective cohort study

Dengbin Guo[1]
Fujian Medical University
Zhenbao Lu[1]
Fujian Medical University
Zhen Lin[1]
Fujian Medical University
Qingping Liu[1]
Fujian Medical University
Kangming Ruan[1]
Fujian Medical University
Dongke Lai[1]
Fujian Medical University
Xi Wang[1]
Fujian Medical University
Xiaoliang Chen[1]
hikki1903@gmail.com
Fujian Medical University

Research Article

Keywords: calcaneal fracture, computed tomography, percutaneous fixation, posterior facet, three-dimensional planning, virtual reduction

Posted Date: November 1st, 2026

DOI: https://doi.org/10.21203/rs.3.rs-11011883/v1

License: This work is licensed under a Creative Commons Attribution 4.0 International License.
Read Full License

Additional Declarations: No competing interests reported.

Abstract

Background

Percutaneous calcaneal fixation does not permit direct visualization of the posterior facet. We examined whether computed tomography (CT)-based three-dimensional (3D) virtual planning was associated with less residual posterior-facet displacement than conventional multiplanar CT planning.

Methods

This retrospective single-center cohort included 85 patients (90 feet) with closed Sanders type II or III fractures treated from March 2020 to February 2025. CT-based 3D virtual planning was used for 42 feet, and conventional multiplanar CT planning was used for 48. Two observers measured posterior-facet step-off and gap on CT obtained 1–3 days after surgery. Patient-clustered generalized estimating equations adjusted for baseline displacement, fracture characteristics, demographic variables, surgical year, and surgeon. Holm correction was applied across the two main imaging outcomes.

Results

Mean step-off was 1.85 ± 0.32 mm after 3D planning and 2.24 ± 0.37 mm after conventional planning. The adjusted difference was − 0.40 mm (95% CI − 0.53 to − 0.28). Mean gap was 1.75 ± 0.33 mm and 2.37 ± 0.50 mm, respectively, with an adjusted difference of − 0.63 mm (95% CI − 0.78 to − 0.47). Both Holm-adjusted P values were < 0.001. Sensitivity analyses, including restriction to observed propensity-score common support, yielded estimates in the same direction. The intraclass correlation coefficient for a single rating, ICC(2,1), was 0.958 for step-off and 0.974 for gap.

Conclusions

Among selected complete cases who completed percutaneous fixation, CT-based 3D virtual planning was associated with 0.40-mm less step-off and 0.63-mm less gap than conventional planning. Nonrandom allocation, time-dependent adoption, and post-entry exclusions preclude causal interpretation. The clinical importance of these submillimetre early imaging differences and any long-term functional or safety benefit remain uncertain.

Trial registration

Not applicable. This was a retrospective observational study in which the investigators did not assign the planning strategy.

Background

Displaced intra-articular calcaneal fractures (DIACFs) disrupt the posterior facet and can reduce calcaneal height and widen the lateral wall [1, 2]. Residual posterior-facet incongruity on postoperative computed tomography (CT) has been associated with limited subtalar motion, pain, and poorer function

[3–5]. In a multicenter randomized trial, patients with a more satisfactory postoperative reduction had better functional outcomes [6]. Restoring posterior-facet congruity and measuring it reliably are therefore central to operative treatment.

Minimally invasive fixation is generally associated with fewer wound complications than extensile lateral open fixation, although most comparative evidence is nonrandomized [7, 8]. Limited exposure, however, makes reduction and screw placement dependent on two-dimensional (2D) fluoroscopy. In a cadaveric Sanders type IIB model, fluoroscopy detected articular malreduction with 63% sensitivity and medial-wall screw penetration with 25% sensitivity [9]. Intraoperative 3D imaging prompted re-reduction in 13 of 62 clinical fractures after standard fluoroscopic views appeared satisfactory [10]. Another consecutive series found at least 2 mm of residual displacement on postoperative CT in 28% of 92 fractures [11]. Thus, satisfactory fluoroscopy does not exclude residual displacement or implant malposition [9–11].

Computer-assisted planning combines patient-specific 3D reconstruction, virtual reduction, implant selection, and simulated screw trajectories [12]. A review identified 79 clinical studies, including 21 controlled studies used to assess efficacy. Pooled estimates favored computer-assisted planning for operative time, blood loss, and fluoroscopy frequency. Reduction quality could not be pooled because outcome definitions differed substantially [12]. The evidence therefore spans heterogeneous anatomical sites and planning systems.

Calcaneal studies have evaluated patient-specific models, printed guides, patient-specific instruments, 3D-printing-assisted fixation, robot-assisted screw placement, virtual reduction, and simulated sustentacular trajectories [13–20]. Most focused on feasibility, operative efficiency, radiographic alignment, function, or implant position. To our knowledge, none directly compared the two planning strategies using standardized early CT measurements of step-off and gap by independent observers whose group labels and study hypothesis were concealed [13, 15–20].

Evidence from other anatomical regions indirectly supports virtual planning and guided fixation [21–26], but differences in anatomy, exposure, fixation targets, and imaging endpoints limit its application to DIACFs. A multicenter randomized trial in calcaneal fracture surgery compared additional intraoperative 3D fluoroscopy with conventional 2D fluoroscopy [27]. Early postoperative CT was assessed by three independent, blinded observers. Although 3D imaging prompted intraoperative correction in 56% of patients, postoperative reduction and fixation quality did not improve [27]. Intraoperative 3D imaging and fracture-specific preoperative planning should therefore be treated as different interventions. Whether virtual reduction and screw-trajectory planning improve early posterior-facet congruity remains uncertain.

We compared CT-based 3D virtual planning with conventional planning in Sanders type II or III DIACFs treated by the same percutaneous approach. The 3D workflow used fracture segmentation, virtual reduction, and screw-trajectory planning; conventional planning used radiographs and multiplanar CT without segmentation or virtual reduction. After data collection, we finalized a non-preregistered analysis plan before dataset lock and designated residual posterior-facet step-off and gap on CT obtained 1–3

days after surgery as the two main imaging outcomes. Group labels, planning records, and the study hypothesis were concealed from the two observers, although postoperative implant configuration could have suggested group assignment. We tested whether both measures were smaller after 3D planning.

Methods

Study design and ethics

We conducted a retrospective cohort study at Affiliated Mindong Hospital, Fujian Medical University. The source population comprised patients who underwent calcaneal fracture surgery from March 2020 to February 2025. Two orthopedic surgeons who had not performed the index operations independently screened the records. They resolved disagreements by consensus. Reporting follows the Strengthening the Reporting of Observational Studies in Epidemiology (STROBE) statement [28]. Additional file 1 contains the completed cohort-study checklist.

The study protocol was approved by the Institutional Review Board of the Affiliated Mindong Hospital of Fujian Medical University (IRB No. K2026083101). The requirement for informed consent to participate was waived by the same Institutional Review Board because the study was retrospective and used de-identified clinical and imaging data collected during routine care. All access to source records and images, data extraction, and formal analysis occurred within the period and scope authorized by the approval. The study was conducted in accordance with the Declaration of Helsinki.

Study population

Patients were eligible if they were 18–70 years old, had a closed Sanders type II or III fracture on preoperative coronal CT, and underwent percutaneous cannulated-screw fixation within 21 days of injury. The analyzed complete-case cohort also required interpretable thin-slice CT before surgery, CT on postoperative days 1–3, complete planning and covariate records, and at least 12 months of follow-up. The late-follow-up requirement supported exploratory longitudinal outcomes but unnecessarily narrowed the cohort available for the early imaging outcomes. The reported estimand is therefore the adjusted between-group difference among feet that completed percutaneous fixation and met all complete-case criteria; it is not an intention-to-treat or pathway-entry effect. Both feet were included for patients with bilateral fractures.

Patients were excluded for an open or pathological fracture; Sanders type I or IV injury; or previous ipsilateral foot or ankle fracture, deformity, or surgery. Other exclusions were an ipsilateral injury affecting imaging or function, neurovascular injury, compartment syndrome, conversion to open reduction or plate fixation, or incomplete records.

Ninety-four patients (99 feet) entered the intended percutaneous-fixation pathway. Nine patients (9 feet) were later excluded: 4 underwent open reduction or plate fixation, 2 lacked planning records, and 3 had

complete baseline and early postoperative CT data but lacked the required late follow-up. The clinical exclusion reason for those three feet was missing late follow-up; however, planning allocation was unavailable in the dataset supplied for this reanalysis for all nine excluded feet. Because the post-entry exclusions included treatment conversions and were not aligned with the timing of the main imaging outcomes, they may have introduced selection bias. The analyzed cohort included 39 patients (42 feet) in the 3D-planning group and 46 patients (48 feet) in the conventional-planning group.

Exposure definition and group allocation

The exposure was the planning method used for the index operation. Allocation was not random and reflected fracture morphology, availability of the digital workflow, and surgeon judgment. The methods overlapped in calendar time, but 3D planning became more common later in the study. Surgical year and operating surgeon were included as covariates to reduce measured confounding by temporal change and surgeon composition; this adjustment cannot remove unmeasured confounding or fully separate the planning method from learning-curve and workflow changes.

Preoperative planning

The center-specific 3D planning workflow used thin-slice preoperative CT as its input. A trained orthopedic surgeon and the operating surgeon jointly completed three mandatory steps for every 3D-planned foot: segmentation of the major fragments, virtual reduction, and screw templating in Mimics 21.0 (Materialise NV, Leuven, Belgium). Slice thickness was 0.625–1.0 mm, and files used Digital Imaging and Communications in Medicine format. Segmented fragments comprised the posterior facet, calcaneal tuberosity, anterior process, and sustentaculum tali. Virtual reduction used the sustentaculum tali and talar articular surface as references and reproduced the operative sequence: traction to restore length, elevation of the posterior facet, correction of lateral-wall widening, and adjustment of hindfoot alignment. Reduction was accepted when posterior-facet step-off was < 1 mm, Gissane angle was 120–145°, and Böhler angle was 25–35°.

The workflow produced a planned fragment alignment and a set of screw entry points, trajectories, lengths, and support configurations. After the operating surgeon accepted the virtual reduction, digital models of 4.0–6.5-mm cannulated screws were positioned to support the posterior facet, sustentaculum tali, and calcaneal tuberosity. The final plan remained visible at the operating-room workstation, but intraoperative adjustment was allowed. No printed guide, navigation system, or postoperative CT data were used. All 42 feet received all three mandatory planning steps (Fig. 1). Planning time, segmentation thresholds and revisions, reasons for intraoperative deviation, and plan-to-implant concordance were not recorded as structured variables. The exposure should therefore be interpreted as a center-specific composite workflow rather than the isolated effect of one software module.

For conventional planning, surgeons reviewed lateral and axial radiographs and multiplanar CT reconstructions in the picture archiving and communication system. They did not segment fragments, perform virtual reduction, or create 3D screw templates. Both groups reviewed preoperative CT; only the 3D group used segmentation, virtual reduction, and simulated screw trajectories.

Surgical technique

The same surgical team, comprising the department director and two senior attending surgeons, treated both groups. General or spinal anesthesia was used, and patients were placed in the lateral decubitus position with the injured side uppermost. A Steinmann pin inserted percutaneously into the calcaneal tuberosity served as a joystick under lateral, axial, and Brodén fluoroscopy. Longitudinal traction restored length and hindfoot alignment. A Kirschner wire or periosteal elevator then elevated the posterior facet using an Essex-Lopresti maneuver. Compression or reduction forceps corrected lateral-wall widening.

After fluoroscopic confirmation of reduction, guidewires were inserted and 4.0-6.5-mm cannulated compression screws were placed percutaneously. Three to five screws were configured according to fracture morphology to support the posterior facet, sustentaculum tali, and calcaneal tuberosity. Surgeons followed the planned entry points, trajectories, and lengths when feasible in the 3D group. Intraoperative adjustment remained permissible. In the conventional group, preoperative imaging and intraoperative fluoroscopy guided screw placement.

Postoperative management and follow-up

Both groups followed the same institutional protocols for perioperative analgesia, 24-h antibiotic prophylaxis, and thromboprophylaxis. Active toe and ankle range-of-motion exercises began on postoperative day 1. Weight bearing was avoided for 6 weeks and was then advanced according to radiographic healing and clinical assessment.

Thin-slice CT of the operated foot was obtained on postoperative days 1–3. The interval was recorded by calendar day, not by hour. Follow-up was scheduled at 6 weeks, 3 months, 6 months, 12 months, and annually thereafter. Follow-up data were abstracted retrospectively from records created during routine clinical care. Clinic nurses who did not participate in the index operation recorded the available assessments. Final assessments occurred in person or by telephone, but the mode was not retained as a structured variable.

Outcomes

The two main imaging outcomes were residual step-off and residual gap of the posterior facet on CT obtained on postoperative days 1–3. Residual step-off was the maximum vertical offset between adjacent articular surfaces. Residual gap was the maximum separation between adjacent articular

margins measured along the articular plane. These measures represent different components of residual displacement and were analyzed separately.

The mean of the two observers was also classified as ≤ 2 mm or > 2 mm. We selected 2 mm as an exploratory imaging threshold because it was the most common cutoff in the cited postoperative CT studies [3, 4, 29]. Published thresholds range from 1 to 3 mm, and no consensus minimal clinically important difference exists. The proportions meeting the threshold for step-off and gap were separate secondary outcomes. These categorical analyses were exploratory and were not interpreted as patient-centered treatment effects. Sensitivity analyses repeated the classification at 1.0, 1.5, 2.0, 2.5, and 3.0 mm.

Secondary outcomes included operative time, blood loss, fluoroscopic exposures, hospital stay, screw number, Böhler angle, Gissane angle, calcaneal height and width, pain, and complications. Pain at rest in the affected foot was recorded on a 0–10 scale, where 0 indicated no pain and 10 the worst imaginable pain. Scores were recorded at 3 months, 6 months, and final follow-up, with each foot scored separately in bilateral cases. Clinic nurses recorded the assessments in person or by telephone. Because neither a named instrument nor a standardized administration protocol was documented consistently, and assessment mode was not retained, these data are described only as 0–10 pain scores. All pain analyses were exploratory.

American Orthopaedic Foot and Ankle Society (AOFAS) ankle-hindfoot scores [30] were available in the follow-up records but were excluded from between-group analyses. Assessment mode varied between in-person and telephone visits. Documentation of clinician-assessed items was insufficient for independent verification in many records. Item-level source data were incomplete for 12 of 90 feet (13.3%), so the recorded totals could not be reconstructed. The reliability and validity of AOFAS clinical rating systems are also limited [31]. No validated alternative functional outcome was collected consistently. Accordingly, the study focused on imaging outcomes and exploratory 0–10 pain scores.

Recorded complications were wound complications, subtalar-joint screw penetration, loss of reduction, symptomatic post-traumatic subtalar arthritis, and unplanned reoperation. Wound complications comprised superficial infection treated with oral antibiotics or deep infection requiring debridement within 30 days. Screw penetration was defined as a screw thread crossing the posterior facet on postoperative CT. Loss of reduction was a ≥ 2-mm increase in step-off or gap between postoperative CT and the latest follow-up image. Symptomatic arthritis required subtalar pain and radiographic degeneration at final follow-up. Unplanned reoperation included any additional operation related to the index fracture during follow-up. Two research nurses reviewed electronic records and follow-up notes, with disagreements adjudicated by the senior author. Because events were retrospectively extracted and sparse, safety analyses were descriptive.

Imaging assessment

CT measurements were made on a picture archiving and communication system workstation using multiplanar reconstructions with slices ≤ 1 mm thick. The posterior facet was examined in calcaneal-aligned coronal and sagittal planes. When the fracture crossed the facet obliquely, the observers also reviewed a reconstruction along the fracture plane. The maximum displacement across all reviewed planes was retained. Two orthopedic surgeons with more than 5 years of calcaneal-trauma experience measured each scan independently. A written protocol specified landmarks, plane and slice selection, reference-line placement, measurement direction, and handling of blurred or metal-obscured margins. The same protocol was used before surgery. Plane, slice, image identifier, and measurement date were not archived systematically; the database retained only each observer's final maximum values.

Group labels, planning records, and the study hypothesis were concealed from the observers. Preoperative and postoperative scans were shown in random order during separate sessions. Complete masking was impossible because postoperative screw configurations remained visible and could have suggested group assignment. Each observer recorded the maximum step-off and gap to the nearest 0.1 mm (Fig. 2). The mean of the two measurements was used in the main analysis.

Inter-rater reliability was quantified using two-way random-effects, absolute-agreement intraclass correlation coefficients. We report a single rating, ICC(2,1), and the mean of two ratings, ICC(2,2), with 95% confidence intervals [32]. Bland–Altman analyses report the mean between-observer difference and 95% limits of agreement. Böhler angle, Gissane angle, calcaneal height, and calcaneal width were measured by one observer; inter-rater reproducibility was therefore not evaluated for these exploratory outcomes.

Statistical analysis

The foot was the unit of analysis, and both feet were retained for five patients with bilateral fractures. Continuous outcome models used robust standard errors clustered by patient. Exploratory binary imaging outcomes used patient-clustered risk differences. Unadjusted Fisher exact tests are shown only as descriptive references because they ignore within-patient correlation. Operative time, blood loss, fluoroscopic exposures, and screw number were recorded per foot. Hospital stay was analyzed once per patient.

Continuous variables are reported as mean ± standard deviation or median (interquartile range), as appropriate. Categorical variables are reported as number (percentage). Baseline distributions were assessed with standardized mean differences (SMDs), without significance tests [33]. No values were missing among variables included in the analyses. Sample size comprised all eligible complete cases during the study period. We did not perform a prospective calculation or an observed post hoc power calculation.

Main imaging analyses

Each main imaging outcome was analyzed with a Gaussian generalized estimating equation using an identity link and exchangeable working correlation. Robust standard errors were clustered by patient. The dependent variable was the postoperative CT measurement. Covariates were planning group, the corresponding preoperative measurement, Sanders type, age, sex, body mass index, time from injury to surgery, preoperative Böhler and Gissane angles, centered surgical year, and operating surgeon. The group coefficient represented 3D minus conventional planning, so negative values indicated smaller residual displacement after 3D planning. Holm correction covered the two-outcome family.

The main model estimated 13 coefficients, including the intercept. Preoperative calcaneal width was omitted to limit overfitting and because its inclusion increased variance inflation factors above 2.5. Estimates changed little after adding width, including both preoperative displacement measures, or using a parsimonious model. The parsimonious model included group, the corresponding preoperative measurement, centered surgical year, and surgeon. Additional file 2 reports the sensitivity analyses.

Sensitivity analyses

Sensitivity analyses used an independent working correlation and modeled surgical year as a six-level categorical variable. Separate analyses excluded the two feet treated in 2025, feet with preoperative step-off ≥ 16 mm, and each surgeon in turn. We also evaluated all 32 possible selections of one foot from each bilateral patient. Propensity scores were estimated at the foot level by unpenalized binary logistic regression with planning group as the dependent variable and age, sex, body mass index, current smoking, diabetes, Sanders type, time from injury to surgery, preoperative Böhler and Gissane angles, and surgical year centered at 2022 as covariates. Conventional planning was the reference, and categorical predictors were indicator coded. Surgeon was not added to this 90-foot propensity model; it was handled by direct adjustment in the outcome models and by surgeon-year sensitivity analyses. Propensity scores were used for overlap diagnostics and post hoc common-support restriction, not for propensity weighting. Observed common support was the intersection of the two group-specific score ranges. Group-specific score summaries and covariate SMDs before and after restriction are reported in Additional file 2. Within the 75-foot subset restricted to surgeon-year strata containing both planning methods, we first repeated the full main outcome-model specification. We then fitted a distinct direct post hoc GEE in the same subset using the corresponding preoperative outcome and fixed effects for the 12 surgeon-year strata, without the other main-model covariates. Observer-specific models used each observer's corresponding preoperative and postoperative measurements with the full main-model covariate set.

Exploratory outcomes

Perioperative, radiographic, pain, and safety outcomes were exploratory. Foot-level continuous outcomes used patient-clustered models, whereas hospital stay was analyzed per patient. Perioperative models adjusted for centered surgical year and surgeon and used an independent generalized estimating equation (GEE) working correlation. Radiographic models also included the corresponding preoperative measure. The longitudinal pain-score model included group, visit, their interaction, preoperative pain

score, centered surgical year, surgeon, and final follow-up month centered at 12 months. The overall group-by-visit interaction was assessed with a two-degree-of-freedom robust Wald test. Benjamini-Hochberg correction was applied separately within the five perioperative, four radiographic, two imaging-threshold, and three visit-specific pain-score families. Sparse complications were described with counts, proportions, and unadjusted risk differences, without confidence intervals or hypothesis tests.

Software and reproducibility

All tests were two-sided. Analyses used the Analysis_Frozen worksheet and Python 3.12.14 with pandas 2.3.3, NumPy 2.5.2, SciPy 1.18.1, statsmodels 0.14.5, and pingouin 0.6.1 where applicable. Versioned scripts were retained for the main models, threshold analyses, and Figs. 4 and 5. The reproducibility archive contains scripts that rerun the 90-foot main GEE models, propensity-score overlap diagnostics, the 80-foot common-support GEE sensitivity analysis, covariate-balance diagnostics, the direct surgeon-year fixed-effect sensitivity analysis, observer-specific contrasts, and the exploratory pain interaction from Analysis_Frozen. The archive exports machine-readable aggregate results but does not reproduce every descriptive table or figure and does not contain the clinical workbook. The non-preregistered, post-data-collection analysis plan was completed on 1 September 2026, before the final analysis was locked. The dataset was frozen on 5 September 2026. Database metadata were revised on 9 September to clarify variable labels and derived follow-up dates; the 90-row Analysis_Frozen values were unchanged. Calcaneal-width, propensity-score common-support, balance, observer-specific, pain-interaction, and surgeon-year analyses added during manuscript preparation are identified as post hoc or exploratory. The analyses should therefore be interpreted as observational and non-confirmatory. During manuscript preparation, OpenAI Codex was used for language editing, document formatting, and assistance in generating reproducible analysis code. It was not used for data collection or clinical decision-making. The authors retain responsibility for the content, analyses, and conclusions.

Results

Cohort construction and participant characteristics

We screened 112 patients (117 feet) and excluded 18 patients (18 feet) at eligibility screening. Ninety-four patients (99 feet) then entered the intended percutaneous-fixation pathway, after which 9 patients (9 feet) were excluded: 4 after conversion to open reduction or plate fixation, 2 because planning records were unavailable, and 3 because the prespecified late-follow-up requirement was not met despite available baseline and early CT data. Missing late follow-up was the clinical exclusion reason for these three feet, but planning allocation for all nine post-entry exclusions was unavailable in the dataset supplied for this reanalysis. The analyzed cohort comprised 39 patients (42 feet) in the 3D-planning group and 46 patients (48 feet) in the conventional-planning group (Fig. 3).

The patient-level mean age was 50.1 ± 7.4 years, and 59 of 85 patients (69.4%) were male. Seventy-one feet (78.9%) had Sanders type II fractures and 19 (21.1%) had type III fractures. Mean time from injury to surgery was 5.8 ± 2.6 days. Postoperative CT was performed after a mean of 2.7 ± 0.5 days.

Several participant and fracture characteristics differed between groups (Table 1). The largest imbalance was surgical year (SMD 0.63), followed by calcaneal width (SMD − 0.36), body mass index (SMD 0.30), preoperative gap (SMD 0.26), and sex (SMD − 0.21). Use of 3D planning rose over time. Annual numbers of 3D-planned feet from 2020 through 2025 were 4, 6, 10, 11, 10, and 1; corresponding conventional counts were 13, 12, 9, 9, 4, and 1. Absolute group SMDs for the three surgeons were ≤ 0.24. Multivariable adjustment could not exclude residual confounding.

Table 1
Participant, fracture, treatment-timing, and follow-up characteristics by planning group

Characteristic / measure	3D planning (39 patients/42 feet)	Conventional planning (46 patients/48 feet)	SMD
Patients / feet	39 / 42	46 / 48	—
Age (years, mean ± SD)*	50.6 ± 8.0	49.7 ± 6.9	0.12
Male, n (%)*	25 (64.1)	34 (73.9)	−0.21
BMI (kg/m², mean ± SD)*	23.6 ± 4.0	22.7 ± 2.0	0.30
Smoking, n (%)*	10 (25.6)	14 (30.4)	−0.11
Diabetes, n (%)*	4 (10.3)	4 (8.7)	0.05
Left side, feet (%)†	20 (47.6)	23 (47.9)	−0.01
Fall from height, feet (%)†	41 (97.6)	46 (95.8)	0.10
Sanders type III, feet (%)†	8 (19.0)	11 (22.9)	−0.10
Time to surgery (days)†	5.7 ± 3.3	5.9 ± 1.8	−0.06
Preoperative step-off (mm)†	5.56 ± 4.25	6.14 ± 4.10	−0.14
Preoperative gap (mm)†	3.70 ± 1.21	3.42 ± 0.95	0.26
Preoperative Böhler angle (°)†	15.1 ± 9.9	13.6 ± 7.7	0.16
Preoperative Gissane angle (°)†	117.2 ± 11.9	115.1 ± 13.4	0.16
Preoperative calcaneal width (mm)†	35.6 ± 5.3	37.3 ± 4.1	−0.36
Preoperative pain score (0–10)†	6.7 ± 1.3	7.0 ± 1.4	−0.20
Follow-up duration (months)†	13.6 ± 1.6	13.7 ± 1.7	−0.05
Postoperative CT interval (days)†	2.69 ± 0.52	2.65 ± 0.53	0.08
Surgical year†	2022.5 ± 1.3	2021.6 ± 1.5	0.63
Surgeon A, feet (%)†	21 (50.0)	24 (50.0)	0.00
Surgeon B, feet (%)†	13 (31.0)	10 (20.8)	0.23
Surgeon C, feet (%)†	8 (19.0)	14 (29.2)	−0.24

BMI, body mass index; CT, computed tomography; SD, standard deviation; SMD, standardized mean difference. * Patient-level data (39 vs. 46 patients). † Foot-level data (42 vs. 48 feet). No significance tests were performed for baseline characteristics. SMDs were calculated using the standard pooled-variance definition for continuous variables and the standard pooled-proportion definition for binary variables.

Exploratory perioperative outcomes

All five perioperative measures were lower after 3D planning (Table 2). Adjusted differences were − 23.16 min for operative time, − 15.48 mL for blood loss, − 7.67 fluoroscopic exposures, − 3.27 days for hospital stay, and − 0.72 screws. Planning time was not recorded, so these findings do not show lower total treatment time or cost. Temporal adoption and concurrent workflow changes may also explain part of the differences.

Table 2
Exploratory perioperative outcomes

Outcome	3D planning (n = 42 feet)	Conventional planning (n = 48 feet)	Adjusted difference (95% CI)	Model P / BH-adjusted q
Operative time (min)	61.5 ± 16.2	84.4 ± 24.2	−23.16 (− 32.48 to − 13.83)	< 0.001 / <0.001
Blood loss (mL)	13.1 ± 9.9	27.7 ± 14.9	−15.48 (− 21.22 to − 9.74)	< 0.001 / <0.001
Fluoroscopic exposures	7.7 ± 1.7	15.5 ± 3.7	−7.67 (− 8.76 to − 6.57)	< 0.001 / <0.001
Hospital stay (days)*	11.5 ± 4.7 (n = 39 patients)	14.8 ± 4.5 (n = 46 patients)	−3.27 (− 5.34 to − 1.20)	0.002 / 0.002
Number of screws	3.6 ± 0.7	4.3 ± 0.7	−0.72 (− 1.02 to − 0.43)	< 0.001 / <0.001

Differences are for 3D minus conventional planning. Foot-level models used an independent GEE working correlation, patient-clustered robust standard errors, and adjustment for surgical year and surgeon. * Hospital stay was analyzed once per patient using linear regression adjusted for surgical year and surgeon. The final column reports the model P value and the BH-adjusted q value within the five-outcome family. BH, Benjamini-Hochberg; CI, confidence interval; GEE, generalized estimating equation. Operative time was recorded from skin incision to final suture; blood loss was estimated from suction volume and gauze weighing; fluoroscopic exposures were counted as each pedal activation of the fluoroscopy unit; hospital stay was counted from the day of surgery to discharge.

Main imaging outcomes: early postoperative CT displacement

Mean postoperative step-off was 1.85 ± 0.32 mm after 3D planning and 2.24 ± 0.37 mm after conventional planning. The adjusted difference was − 0.40 mm (95% CI − 0.53 to − 0.28; Holm-adjusted P < 0.001). Mean gap was 1.75 ± 0.33 mm and 2.37 ± 0.50 mm, respectively; the adjusted difference was

− 0.63 mm (95% CI − 0.78 to − 0.47; Holm-adjusted P < 0.001; Table 3; Fig. 4). These estimates describe association within the selected complete-case cohort and do not establish a causal effect.

A step-off ≤ 2 mm was observed in 31 of 42 feet (73.8%) after 3D planning and 13 of 48 (27.1%) after conventional planning. For gap, the corresponding counts were 35 of 42 (83.3%) and 13 of 48 (27.1%). Patient-clustered risk differences were 46.7 percentage points (95% CI 28.5 to 65.0) for step-off and 56.3 points (95% CI 39.1 to 73.4) for gap. Differences were largest at intermediate thresholds between 1.0 and 3.0 mm; neither group met the 1.0-mm threshold. These threshold-dependent results do not define a patient-important benefit.

Adjusted estimates remained negative in sensitivity analyses of working correlation, calendar year, surgeon, and bilateral fractures (Additional file 2). Propensity scores ranged from 0.216 to 0.868 after 3D planning and from 0.119 to 0.816 after conventional planning; observed common support was 0.216 to 0.816. Restriction retained 80 feet from 77 patients (41 3D planning and 39 conventional planning), with adjusted differences of − 0.40 mm (95% CI − 0.53 to − 0.28) for step-off and − 0.61 mm (95% CI − 0.77 to − 0.45) for gap. Covariate balance improved for most propensity-model variables, but residual SMDs were 0.38 for surgical year, 0.22 for body mass index, and 0.24 for preoperative Böhler angle. Within the separate 75-foot surgeon-year overlap subset, repeating the full main covariate model yielded adjusted differences of − 0.35 mm (95% CI − 0.48 to − 0.21) for step-off and − 0.59 mm (95% CI − 0.76 to − 0.42) for gap. The distinct direct model using the corresponding baseline outcome and 12 surgeon-year stratum indicators yielded − 0.41 mm (95% CI − 0.55 to − 0.28) and − 0.55 mm (95% CI − 0.72 to − 0.39), respectively. These post hoc restrictions addressed narrower populations and did not remove unmeasured confounding.

Table 3
Early postoperative CT outcomes

Outcome	3D (n = 42)	Conventional (n = 48)	Unadjusted estimate (95% CI)	Adjusted estimate* (95% CI)	Multiplicity-adjusted value
Postoperative step-off, mm	1.85 ± 0.32	2.24 ± 0.37	−0.40 (− 0.54 to − 0.25)	−0.40 (− 0.53 to − 0.28)	< 0.001 (Holm P)
Postoperative gap, mm	1.75 ± 0.33	2.37 ± 0.50	−0.61 (− 0.79 to − 0.44)	−0.63 (− 0.78 to − 0.47)	< 0.001 (Holm P)
Step-off ≤ 2 mm, n (%)	31 (73.8)	13 (27.1)	RD 46.7% (28.5 to 65.0)	—	< 0.001 (BH q)
Gap ≤ 2 mm, n (%)	35 (83.3)	13 (27.1)	RD 56.3% (39.1 to 73.4)	—	< 0.001 (BH q)

* Continuous outcomes used patient-clustered Gaussian GEE with exchangeable working correlation and adjustment for the corresponding preoperative value, Sanders type, age, sex, body mass index, time to surgery, preoperative Böhler and Gissane angles, centered surgical year, and surgeon. The displayed P

values for the two main imaging outcomes are Holm adjusted. Binary outcomes are exploratory; the unadjusted risk differences (RDs) shown in the unadjusted-estimate column were estimated using Gaussian GEE with an identity link, independent working correlation, and patient-clustered robust standard errors. BH-adjusted q values for the two patient-clustered RDs were < 0.001. Fisher exact P values were calculated only for descriptive reference and do not account for within-patient correlation. BH, Benjamini–Hochberg; CI, confidence interval; CT, computed tomography; GEE, generalized estimating equation; RD, risk difference.

Inter-rater agreement

Agreement between observers was high. ICC(2,1) was 0.958 (95% CI 0.94–0.97) for step-off and 0.974 (95% CI 0.96–0.98) for gap. ICC(2,2) was 0.979 (95% CI 0.97–0.99) and 0.987 (95% CI 0.98–0.99), respectively. Mean between-observer differences were − 0.009 mm for step-off and − 0.012 mm for gap; the corresponding 95% limits of agreement were − 0.238 to 0.220 mm and − 0.249 to 0.224 mm. Observer-specific adjusted differences were similar: −0.40 and − 0.41 mm for step-off and − 0.61 and − 0.65 mm for gap (Additional file 2). Three step-off measurements and four gap measurements lay outside the limits (Fig. 5).

Exploratory radiographic outcomes

After adjustment for the preoperative measure, surgical year, and surgeon, the 3D-planning group had a larger postoperative Böhler angle (2.46°, 95% CI 0.15–4.77; BH q = 0.049). Adjusted differences were also observed for Gissane angle (3.66°, 95% CI 0.35–6.98; q = 0.049) and calcaneal height (1.53 mm, 95% CI 0.52–2.53; q = 0.011). Calcaneal width differed by 0.34 mm (95% CI − 1.07 to 1.74; q = 0.637). These single-observer outcomes were exploratory, and no threshold for clinical importance was prespecified.

Exploratory pain outcomes

Recorded 0–10 pain scores were lower in the 3D-planning group at 3 months, 6 months, and final follow-up (Table 4). Adjusted differences were − 0.95 (95% CI − 1.57 to − 0.34), − 0.94 (95% CI − 1.43 to − 0.44), and − 0.66 (95% CI − 1.09 to − 0.23), respectively. The overall group-by-visit interaction was not conclusive (robust Wald χ^2=5.84, 2 df, P = 0.054); the visit-specific contrasts are therefore interpreted descriptively. Because the instrument and administration mode were documented inconsistently, these exploratory estimates do not establish a validated patient-reported benefit or show that early CT differences caused later pain differences.

Table 4
Exploratory 0–10 pain outcomes

Outcome	3D planning (n = 42)	Conventional planning (n = 48)	Adjusted difference (95% CI)*	Model P / BH-adjusted q
Pain score at 3 months	3.6 ± 1.4	4.5 ± 1.4	−0.95 (− 1.57 to − 0.34)	0.002 / 0.003
Pain score at 6 months	2.0 ± 1.1	2.9 ± 1.2	−0.94 (− 1.43 to − 0.44)	< 0.001 / <0.001
Pain score at final follow-up	1.1 ± 0.9	1.7 ± 0.9	−0.66 (− 1.09 to − 0.23)	0.003 / 0.003

* Longitudinal Gaussian GEE with patient clustering and exchangeable working correlation, adjusted for preoperative pain score, centered surgical year, surgeon, and final follow-up month. Differences are for 3D minus conventional planning. The final column reports the model P value and the BH-adjusted q value within the three-contrast family. BH, Benjamini-Hochberg; CI, confidence interval; GEE, generalized estimating equation.

Note

Recorded AOFAS ankle-hindfoot totals were excluded because assessment mode varied and item-level source data could not be reconstructed (see Outcomes in Methods).

Complications

At least one complication was recorded in 5 of 42 feet (11.9%) after 3D planning and 13 of 48 feet (27.1%) after conventional planning. The descriptive unadjusted risk difference was − 15.2 percentage points (Table 5). Events were sparse and were mapped retrospectively from unstructured records to prespecified categories. We therefore make no comparative safety inference.

Table 5
Recorded complications

Complication	3D planning (n = 42)	Conventional planning (n = 48)	Risk difference (percentage points)
Wound complication	2 (4.8)	6 (12.5)	−7.7
Subtalar-joint screw penetration	1 (2.4)	0 (0)	2.4
Loss of reduction	1 (2.4)	4 (8.3)	−6.0
Post-traumatic subtalar arthritis	1 (2.4)	3 (6.2)	−3.9
Unplanned reoperation	2 (4.8)	0 (0)	4.8
Any complication	5 (11.9)	13 (27.1)	−15.2

Values are number of feet (%). Risk differences are unadjusted percentage-point differences calculated as 3D minus conventional planning. Events were summarized descriptively because they were sparse and bilateral feet were not independent; no inferential confidence intervals or hypothesis tests are presented. Event categories are not mutually exclusive; a single foot could contribute to more than one category. "Any complication" was defined as the union of all recorded events per foot and deduplicated at the foot level.

Discussion

Within the selected complete-case cohort, CT-based 3D virtual planning was associated with less residual posterior-facet step-off and gap after the same percutaneous fixation approach. The submillimetre differences were measured on early CT. Nonrandom allocation, increasing use of 3D planning over time, and post-entry exclusions preclude causal or clinical conclusions.

Most comparative studies of calcaneal fractures have examined fixation constructs or operative approaches rather than preoperative planning. Chang et al. compared minimally invasive locking plates with screw fixation through a sinus tarsi approach [34]. Their retrospective study used functional outcomes and plain radiographic measures of reduction maintenance. Chen et al. compared ligamentotaxis-assisted percutaneous fixation with extensile lateral plate fixation [35]. Although they obtained immediate postoperative CT, subsequent assessment relied mainly on radiographs. Neither study reported independent, blinded continuous measurements of posterior-facet step-off and gap. Neither directly tested virtual planning within a uniform percutaneous fixation framework.

Finite element studies offer biomechanical plausibility but not clinical evidence. Peng et al. found lower modeled stress and interfragmentary displacement when a medial longitudinal screw reached the sustentaculum tali [36]. Li et al. reported lower fragment stress and displacement for frame-

configuration screw constructs than for plate fixation under static axial loading [37]. Both studies used idealized models derived from one healthy adult. Their results support attention to screw trajectories but cannot establish better intraoperative reduction or postoperative congruity. Our composite workflow also does not isolate the effects of virtual reduction, screw planning, or other components.

Previous calcaneal studies evaluated virtual simulation [19] or screw-trajectory simulation [20] mainly for feasibility. They did not compare achieved early postoperative CT step-off and gap between planning strategies within a uniform percutaneous fixation framework. The present association therefore addresses a narrower imaging question but remains vulnerable to confounding and selection.

The adjusted differences of 0.40 mm for step-off and 0.63 mm for gap should be interpreted as early reduction-quality signals rather than patient-important effects. Published CT thresholds vary, the 2-mm cutoff is exploratory, and no validated minimal clinically important difference exists for these measurements [3, 4, 29]. The findings should not by themselves change clinical practice. Their immediate value is to define a reproducible imaging endpoint and an effect-size range for prospective multicenter studies that also measure validated patient-reported outcomes.

Ma et al. used CT-based 3D reconstruction and simulated reduction to quantify posterior-facet translation and rotation in 71 unilateral Sanders type II or III fractures [39]. That study provided anatomical information relevant to virtual reduction but did not compare planning strategies or achieved postoperative congruity. Our study instead examined whether a center-specific planning workflow was associated with early postoperative CT reduction.

A related cohort from our institution applied a similar virtual-reduction and implant-templating workflow to posterolateral tibial plateau fractures [40]. The authors confirmed from institutional cohort records that no patient appeared in both studies. The present study addresses a distinct anatomy, percutaneous approach, and posterior-facet CT endpoint; the earlier study therefore documents workflow transferability rather than validation of the current findings.

Functional comparisons were unavailable because AOFAS assessment modes and clinician-assessed components could not be verified consistently, and item-level data for 12 of 90 feet were insufficient to reconstruct the recorded totals. The exploratory 0–10 pain-score differences do not show that improved reduction mediated symptom relief. Short follow-up and sparse complications also prevent conclusions about long-term joint preservation or comparative safety.

A possible mechanism is that 3D planning lets surgeons rehearse reduction and inspect entry points, trajectories, and screw lengths before entering the operating room, potentially reducing intraoperative adjustments. Planning time, segmentation revisions, deviations from the plan, and reasons for deviation were not recorded, so this mechanism was not tested. The effects of virtual reduction and screw planning cannot be separated. The study therefore evaluates a center-specific composite workflow rather than a transferable software effect, and applicability is limited to teams with similar training, equipment, and case mix.

Temporal confounding is the main threat to validity. Three-dimensional planning was used more often later in the study (surgical-year SMD 0.63). Surgeon experience, team workflow, equipment, and case selection may have changed at the same time. Estimates remained negative in the direct surgeon-year fixed-effect analysis, but adjustment, categorical-year models, and leave-one-surgeon-out analyses cannot remove unmeasured concurrent changes or separate planning from a learning curve.

Propensity-score overlap was incomplete, with 10 feet outside observed common support. Restriction to the 80-foot overlap sample yielded similar estimates but left residual imbalance in surgical year and other covariates. This restriction and the 75-foot surgeon-year analysis changed the target population and did not establish exchangeability. They support the stability of the association under narrower observed comparisons, not a causal treatment effect.

Post-entry exclusions may have introduced selection bias. Four feet were converted to open reduction or plate fixation; of the other five excluded feet, two lacked planning records and three had baseline and early postoperative CT data but not the required late follow-up. Missing late follow-up was the clinical exclusion reason for those three feet, whereas planning allocation for all nine was unavailable in the dataset supplied for this reanalysis. Requiring late follow-up narrowed an analysis whose main outcomes occurred within three days, and the direction and magnitude of any resulting bias cannot be determined from the retained analytic dataset. The findings therefore apply only to patients who completed percutaneous fixation and met the complete-case criteria.

Measurement bias is also possible. Group labels and the study hypothesis were concealed, but observers could see screw configurations. Because the 3D group used fewer screws on average (3.6 vs 4.3), observers might have inferred allocation. Observer-specific adjusted contrasts were similar, and ICC values exceeded 0.95, but these findings show consistency rather than freedom from shared bias or measurement accuracy. Future studies could use standardized, cropped articular images that obscure implants and other group cues, with adjudication by an independent radiologist. One observer measured radiographic morphology, and complications were reconstructed retrospectively without structured event fields. The single-center setting, three surgeons, small cohort, and 12–19 months of follow-up further limit generalizability and safety inference and cannot determine whether early imaging differences persist or improve arthritis, chronic pain, or long-term function.

A prospective multicenter study should enroll patients when the planning strategy is chosen and retain conversions and losses in the target cohort. It should use the present continuous CT measurements and effect-size range for sample-size planning, while recording planning time, segmentation changes, plan-to-implant concordance, surgeon experience, and validated patient-reported outcomes. Longer follow-up is needed to determine whether early imaging differences are causal and clinically important.

Conclusions

Among selected patients with Sanders type II or III fractures who completed percutaneous fixation, CT-based 3D virtual planning was associated with less residual posterior-facet displacement on early CT.

The adjusted differences were smaller than 1 mm, and their clinical importance is uncertain. Selection, temporal confounding, and incomplete masking prevent causal interpretation. Prospective multicenter studies should enroll patients when planning is chosen, retain pathway conversions, and assess validated patient-reported and long-term subtalar outcomes.

Abbreviations

AOFAS
American Orthopaedic Foot and Ankle Society
BH
Benjamini-Hochberg
CI
confidence interval
CT
computed tomography
DIACF
displaced intra-articular calcaneal fracture
GEE
generalized estimating equation
ICC
intraclass correlation coefficient
MCID
minimal clinically important difference
PACS
picture archiving and communication system
RD
risk difference
SD
standard deviation
SMD
standardized mean difference.

Declarations

Ethics approval and consent to participate

The study protocol was approved by the Institutional Review Board of the Affiliated Mindong Hospital of Fujian Medical University (IRB No. K2026083101). The requirement for informed consent to participate was waived by the same Institutional Review Board because the study was retrospective and used de-identified clinical and imaging data collected during routine care. All access to source records and

images, data extraction, and formal analysis occurred within the period and scope authorized by the approval. The study was conducted in accordance with the Declaration of Helsinki.

Consent for publication

Not applicable. Figures 1 and 2 contain only cropped, de-identified CT images with direct identifiers, accession identifiers, and dates removed. No individual can be identified from the submitted images. The authors report that publication of these de-identified images was covered by the Institutional Review Board waiver; separate publication consent was therefore not required.

Competing interests

The authors declare that they have no competing interests.

Funding

No funding was received for this study.

Author Contribution

DG (Dengbin Guo): Conceptualization, Methodology, Investigation, Data curation, Writing – original draft. ZL (Zhen Lin): Methodology, Software, Formal analysis, Visualization, Writing – review and editing. ZBL (Zhenbao Lu), XC (Xiaoliang Chen), QL (Qingping Liu), XW (Xi Wang), and DL (Dongke Lai): Investigation, Writing – review and editing. KR (Kangming Ruan): Resources, Writing – review and editing. All authors read and approved the final manuscript.

Acknowledgements

Not applicable.

Availability of data and materials

The de-identified minimum dataset is not publicly available because it contains clinical treatment information governed by institutional ethics and privacy requirements. It is available from the corresponding author on reasonable request, subject to approval by the responsible ethics and data-governance bodies and safeguards against re-identification. Reproducible analysis code and machine-readable aggregate outputs are provided in Additional file 3.

References

1. Sanders R, Fortin P, DiPasquale T, Walling A. Operative treatment in 120 displaced intraarticular calcaneal fractures. Results using a prognostic computed tomography scan classification. Clin Orthop Relat Res. 1993;29087–95. 10.1097/00003086-199305000-00012.
2. Rammelt S, Zwipp H. Calcaneus fractures: facts, controversies and recent developments. Injury. 2004;35(5):443–61. 10.1016/j.injury.2003.10.006.
3. van Hoeve S, de Vos J, Verbruggen JPAM, Willems P, Meijer K, Poeze M. Gait analysis and functional outcome after calcaneal fracture. J Bone Joint Surg Am. 2015;97(22):1879–88. 10.2106/JBJS.N.01279.
4. Eom JS, Joo YD, Kim SJ, Shin MH, Lee DO, Jung HG. Correlation analysis of reduction for intra-articular calcaneal fracture and clinical outcomes using postoperative computed tomography. J Korean Foot Ankle Soc. 2014;18(4):165–72. 10.14193/jkfas.2014.18.4.165.
5. Ojeda-Jiménez J, Rendón-Díaz D, Martín-Vélez P, González-Martín D, Boluda-Mengod J, Méndez-Ojeda M et al. Surgically treated calcaneal joint fractures: what does postoperative computed tomography give us? Rev Esp Cir Ortop Traumatol (Engl Ed). 2020;64(6):393–400. 10.1016/j.recot.2020.06.001
6. Buckley R, Tough S, McCormack R, Pate G, Leighton R, Petrie D, et al. Operative compared with nonoperative treatment of displaced intra-articular calcaneal fractures: a prospective, randomized, controlled multicenter trial. J Bone Joint Surg Am. 2002;84(10):1733–44. 10.2106/00004623-200210000-00001.
7. Zhang Y, Weng Q, Gu Y, Chen J, Yang Y. Calcaneal fractures: 3D-printing model to assist spatial weaving of percutaneous screws versus conventional open fixation—a retrospective cohort study. Int Orthop. 2021;45(9):2337–46. 10.1007/s00264-021-05094-2.
8. Majeed H, Barrie J, Munro W, McBride D. Minimally invasive reduction and percutaneous fixation versus open reduction and internal fixation for displaced intra-articular calcaneal fractures: a systematic review of the literature. EFORT Open Rev. 2018;3(7):418–25. 10.1302/2058-5241.3.170043.
9. Kendoff D, Citak M, Gardner MJ, Kfuri M Jr, Thumes B, Krettek C, et al. Three-dimensional fluoroscopy for evaluation of articular reduction and screw placement in calcaneal fractures. Foot Ankle Int. 2007;28(11):1165–71. 10.3113/FAI.2007.1165.
10. Eckardt H, Lind M. Effect of intraoperative three-dimensional imaging during the reduction and fixation of displaced calcaneal fractures on articular congruence and implant fixation. Foot Ankle Int. 2015;36(7):764–73. 10.1177/1071100715576518.
11. Chongmuenwai A, Wongfukiat O, Choovongkomol K. Postoperative 3D computed tomographic evaluation of 92 calcaneal fracture reduction using the sinus tarsi technique and fixation with 3.5 mm cortical screws. Eur J Orthop Surg Traumatol. 2024;34(6):2957–62. 10.1007/s00590-024-03998-4.
12. Moolenaar JZ, Tümer N, Checa S. Computer-assisted preoperative planning of bone fracture fixation surgery: a state-of-the-art review. Front Bioeng Biotechnol. 2022;10:1037048.

10.3389/fbioe.2022.1037048.

13. Ozturk AM, Ozer MA, Suer O, Derin O, Govsa F, Aktuglu K. Evaluation of the effects of using 3D-patient specific models of displaced intra-articular calcaneal fractures in surgery. Injury. 2022;53(Suppl 2):S40–51. 10.1016/j.injury.2020.04.057.
14. Yang S, Lin H, Luo C. Meta-analysis of 3D printing applications in traumatic fractures. Front Surg. 2021;8:696391. 10.3389/fsurg.2021.696391.
15. Song Q, Li T, Xia H, Li Y, Feng C, Lin Y, et al. Three-dimensional printed cast assisted screw fixation of calcaneal fractures: a prospective study. BMC Musculoskelet Disord. 2023;24:802. 10.1186/s12891-023-06927-4.
16. Wang C, Xu C, Li M, Li H, Xiao H, Zhong D, et al. Patient-specific instrument-assisted minimally invasive internal fixation of calcaneal fracture for rapid and accurate execution of a preoperative plan: a retrospective study. BMC Musculoskelet Disord. 2020;21:407. 10.1186/s12891-020-03439-3.
17. Miao K, Wang J, Yu K, Hong J, Lu X. Percutaneous reduction and cannulated screw fixation assisted by 3D printing technology of calcaneal fractures in children. J Orthop Sci. 2024;29(1):236–42. 10.1016/j.jos.2022.12.004.
18. Wang J, Han W, Su Y, Wang J, Jiang X. Comparison of robot-assisted percutaneous cannulated screws versus open reduction and internal fixation in calcaneal fractures. Orthop Surg. 2023;15(3):724–30. 10.1111/os.13650.
19. Xia S, Fu B, Wang B, Wu J, Cui Y, Wang X. Computed tomography imaging-based preoperative virtual simulation for calcaneal fractures reduction. J Foot Ankle Surg. 2019;58(2):248–52. 10.1053/j.jfas.2018.08.054.
20. Li X, Wang XK, Yu LK, Zhang C, Zhao MM, Yan J, et al. 3D simulation of percutaneous sustentaculum tali screw insertion in calcaneal fractures. BMC Musculoskelet Disord. 2023;24:636. 10.1186/s12891-023-06748-5.
21. Jia X, Zhang K, Qiang M, Wu Y, Chen Y. Association of computer-assisted virtual preoperative planning with postoperative mortality and complications in older patients with intertrochanteric hip fracture. JAMA Netw Open. 2020;3(8):e205830. 10.1001/jamanetworkopen.2020.5830.
22. Gao H, Liu Z, Bai X, Wang G, Xu G, Ma J, et al. Comparison of freehand technique and a novel laser-guiding navigation system in femoral neck-cannulated screw fixation: a randomized controlled trial. BMC Surg. 2023;23:319. 10.1186/s12893-023-02226-w.
23. Zhao P, Liu L, Chen J, Li R, Wang X, Wu M. An investigation to the clinical application of personalized 3D printed guides combined with preoperative virtual iliosacral screws for the management of posterior pelvic ring injury. BMC Surg. 2025;25:438. 10.1186/s12893-025-03193-0.
24. Tao X, Lyu F, Sugand K, Zhou K, Wang H. Does a novel 3D printed individualized guiding template based on cutaneous fiducial markers contribute to accurate percutaneous insertion of pelvic screws? A preliminary phantom and cadaver study. BMC Surg. 2024;24:105. 10.1186/s12893-024-02402-6.

25. Wu RJ, Zhang W, Lin YZ, Fang ZL, Wang KN, Wang CX, et al. Influence of preoperative simulation on the reduction quality and clinical outcomes of open reduction and internal fixation for complex proximal humerus fractures. BMC Musculoskelet Disord. 2023;24:243. 10.1186/s12891-023-06348-3.
26. Prijs J, Schoolmeesters B, Eygendaal D, de Vries JPPM, Jutte PC, Doornberg JN, et al. 3D virtual preoperative planning may reduce the incidence of dorsal screw penetration in volar plating of intra-articular distal radius fractures. Eur J Trauma Emerg Surg. 2022;48(5):3911–21. 10.1007/s00068-021-01800-2.
27. Halm JA, Beerekamp MSH, de Muinck-Keizer RJ, Beenen LFM, Maas M, Goslings JC, et al. Intraoperative effect of 2D vs 3D fluoroscopy on quality of reduction and patient-related outcome in calcaneal fracture surgery. Foot Ankle Int. 2020;41(8):954–63. 10.1177/1071100720926111.
28. von Elm E, Altman DG, Egger M, Pocock SJ, Gøtzsche PC, Vandenbroucke JP, STROBE Initiative. The Strengthening the Reporting of Observational Studies in Epidemiology (STROBE) statement: guidelines for reporting observational studies. Lancet. 2007;370(9596):1453–7. 10.1016/S0140-6736(07)61602-X.
29. de Muinck Keizer RJO, Beerekamp MSH, Ubbink DT, Beenen LFM, Schepers T, Goslings JC. Systematic CT evaluation of reduction and hardware positioning of surgically treated calcaneal fractures: a reliability analysis. Arch Orthop Trauma Surg. 2017;137(9):1261–7. 10.1007/s00402-017-2744-5.
30. Kitaoka HB, Alexander IJ, Adelaar RS, Nunley JA, Myerson MS, Sanders M. Clinical rating systems for the ankle-hindfoot, midfoot, hallux, and lesser toes. Foot Ankle Int. 1994;15(7):349–53. 10.1177/107110079401500701.
31. Pinsker E, Daniels TR. AOFAS position statement regarding the future of the AOFAS clinical rating systems. Foot Ankle Int. 2011;32(9):841–2. 10.3113/FAI.2011.0841.
32. Koo TK, Li MY. A guideline of selecting and reporting intraclass correlation coefficients for reliability research. J Chiropr Med. 2016;15(2):155–63. 10.1016/j.jcm.2016.02.012.
33. Austin PC. Balance diagnostics for comparing the distribution of baseline covariates between treatment groups in propensity-score matched samples. Stat Med. 2009;28(25):3083–107. 10.1002/sim.3697.
34. Chang YJ, Hsu CH, Liao CC, Kuo FC, Lu YD, Hsu SL, et al. Clinical and radiologic outcomes of minimally invasive locking plate versus screw fixation for displaced intra-articular calcaneal fractures (DIACFs) via sinus tarsi approach: a comparative study. BMC Surg. 2025;25:449. 10.1186/s12893-025-03208-w.
35. Chen Z, Fan C, Zhang J, Zhao C, Du X, Huang W, et al. A novel minimally invasive percutaneous treatment for Essex-Lopresti joint depression-type DIACFs by ligamentotaxis. BMC Surg. 2022;22:431. 10.1186/s12893-022-01868-6.
36. Peng Y, Luo G, Ni W. A finite element analysis of the optimal longitudinal screw trajectory for Sanders II and Sanders III calcaneal fractures fixed with percutaneous screws. BMC Surg.

2025;25:261. 10.1186/s12893-025-02949-y.

37. Li M, Zhang B, Bai X, Song D, Wang B, Chen W. Biomechanical comparison of frame configuration screw fixation and conventional plate fixation for Sanders type III fractures: a finite element analysis. BMC Surg. 2026;26:360. 10.1186/s12893-026-03684-8.
38. Su Y, Chen W, Zhang T, Wu X, Wu Z, Zhang Y. Böhler's angle's role in assessing the injury severity and functional outcome of internal fixation for displaced intra-articular calcaneal fractures: a retrospective study. BMC Surg. 2013;13:40. 10.1186/1471-2482-13-40.
39. Ma X, Zhai S, Zhang S, Shen P, Di L, Chen W, et al. A quantitative three-dimensional analysis of posterior facet displacement in Sanders type II and III intra-articular calcaneal fractures. Front Surg. 2026;13:1839210. 10.3389/fsurg.2026.1839210.
40. Lin J, Lu Z, Zhou S, Lin Y, Lin W, Guo W, et al. CT-based three-dimensional virtual reduction with implant templating for tibial plateau fractures involving the posterolateral region: a retrospective cohort study of early postoperative CT reduction quality. BMC Surg. 2026. 10.1186/s12893-026-04113-6.

Figures

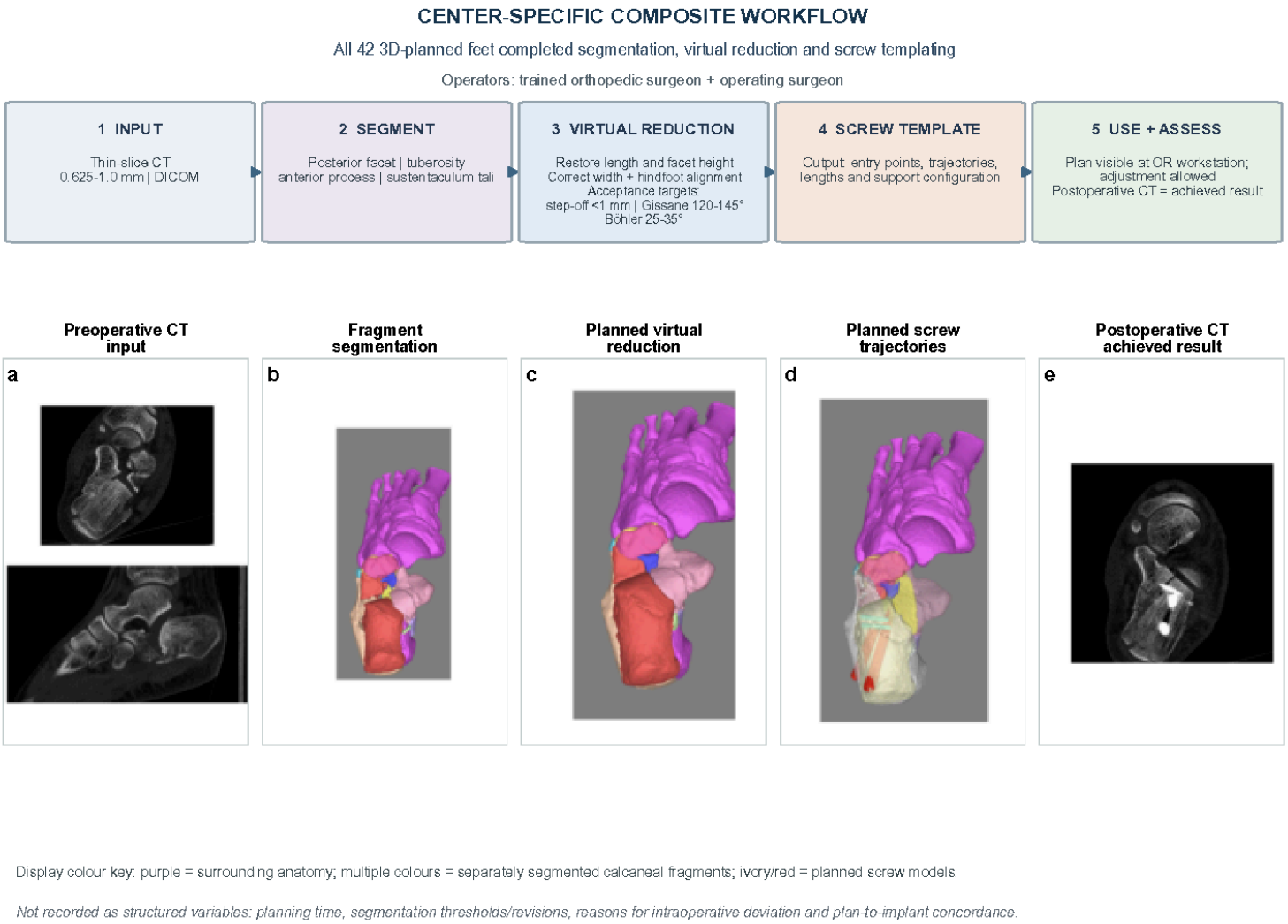
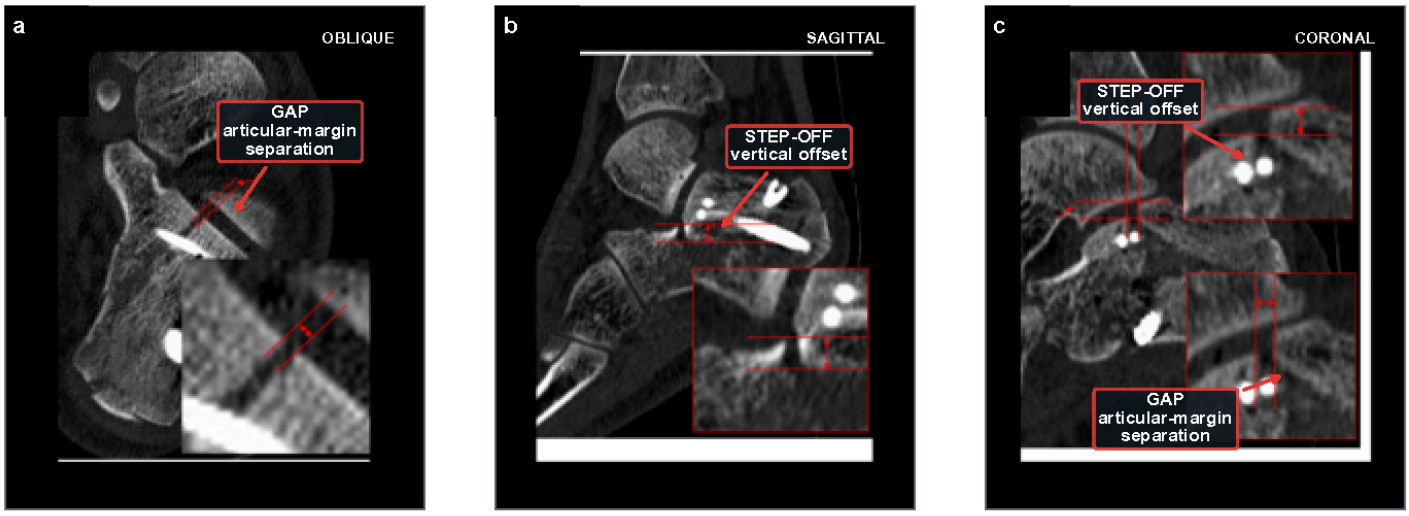


Figure 1

Center-specific CT-based three-dimensional planning workflow. The workflow banner identifies the input, joint operators, mandatory stages completed for all 42 three-dimensional-planned feet, outputs, intraoperative use, and postoperative assessment. (a) Thin-slice preoperative coronal and sagittal CT input. (b) Segmentation of the major fragments. (c) Planned virtual reduction. (d) Planned screw entry points, trajectories, lengths, and support configuration. (e) Postoperative CT showing the achieved reduction; postoperative images were used only for assessment. Display colours distinguish surrounding anatomy, segmented fragments, and planned screw models and do not encode outcome. Planning time, segmentation thresholds and revisions, reasons for intraoperative deviation, and plan-to-implant concordance were not recorded as structured variables.

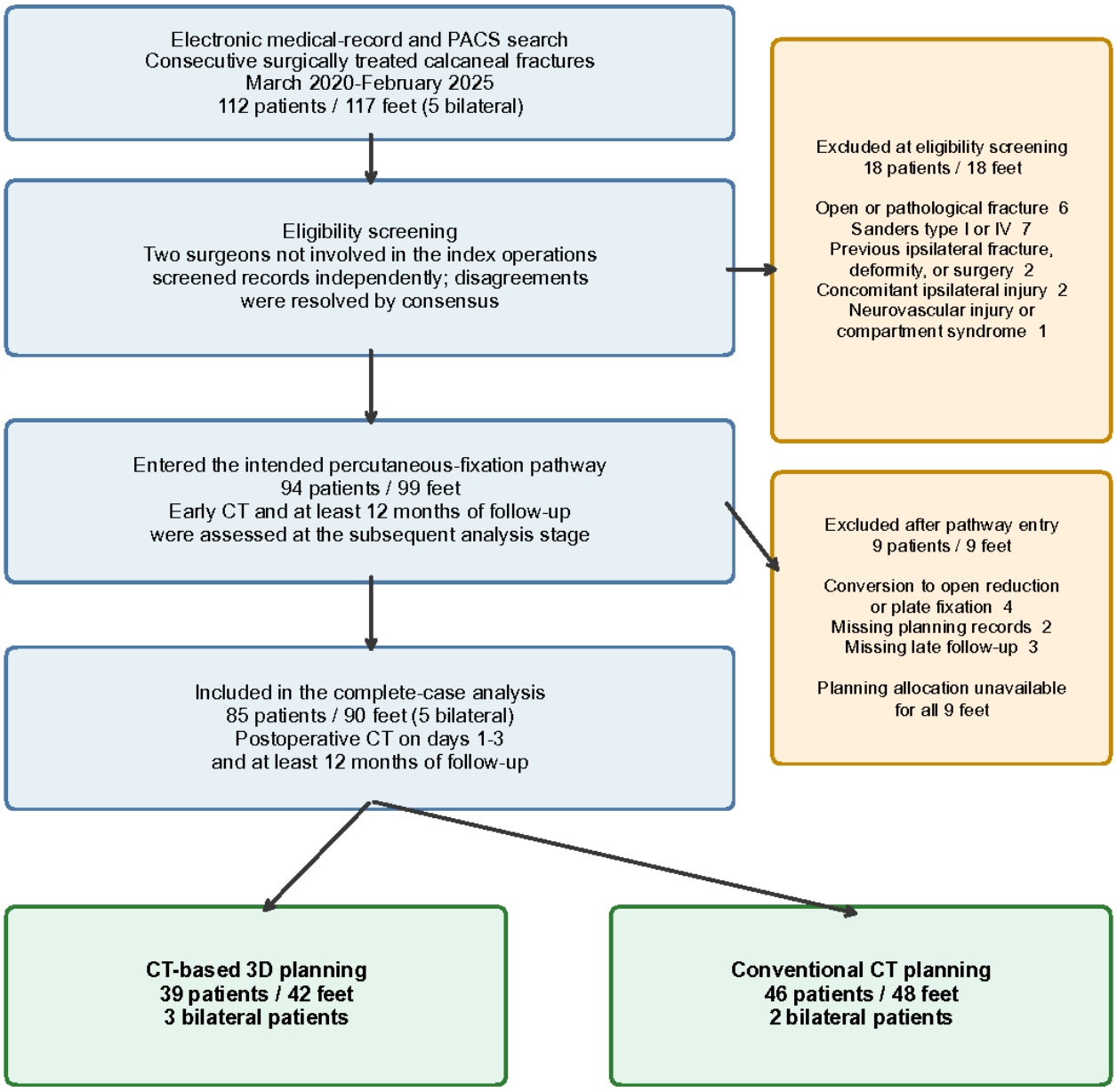


Red double arrows show measurement direction: gap is separation between opposing articular margins; step-off is vertical offset between adjacent articular surfaces.

Scans were randomized and group labels, planning records and the study hypothesis were hidden; postoperative implants remained visible.

Figure 2

CT measurement of posterior-facet displacement. (a) Residual gap on an oblique multiplanar reconstruction aligned to the fracture plane; gap is the separation between opposing articular margins. (b) Residual step-off on a sagittal reconstruction; step-off is the vertical offset between adjacent articular surfaces. (c) Coronal reconstruction from the same case showing both measures. Red double arrows indicate measurement direction. Measurements were obtained in calcaneal-aligned coronal and sagittal planes, with additional oblique planes reviewed when the fracture line traversed the facet obliquely; the maximum value across reviewed planes was retained. Scans were shown in random order, and group labels, planning records, and the study hypothesis were hidden from the observers; postoperative implants remained visible and could have suggested group assignment.



The foot was the analysis unit; inferential models accounted for clustering by patient.

Figure 3

Flow of patients and feet through the study. Ninety-four patients (99 feet) entered the intended percutaneous-fixation pathway; nine patients (nine feet) were subsequently excluded. These comprised four conversions to open reduction or plate fixation, two feet with missing planning records, and three feet whose clinical exclusion reason was missing required late follow-up despite available baseline and early postoperative CT. Planning allocation for all nine was unavailable in the dataset supplied for this

reanalysis. The selected complete-case analysis included 85 patients (90 feet). The foot was the analysis unit; inferential models accounted for clustering by patient.

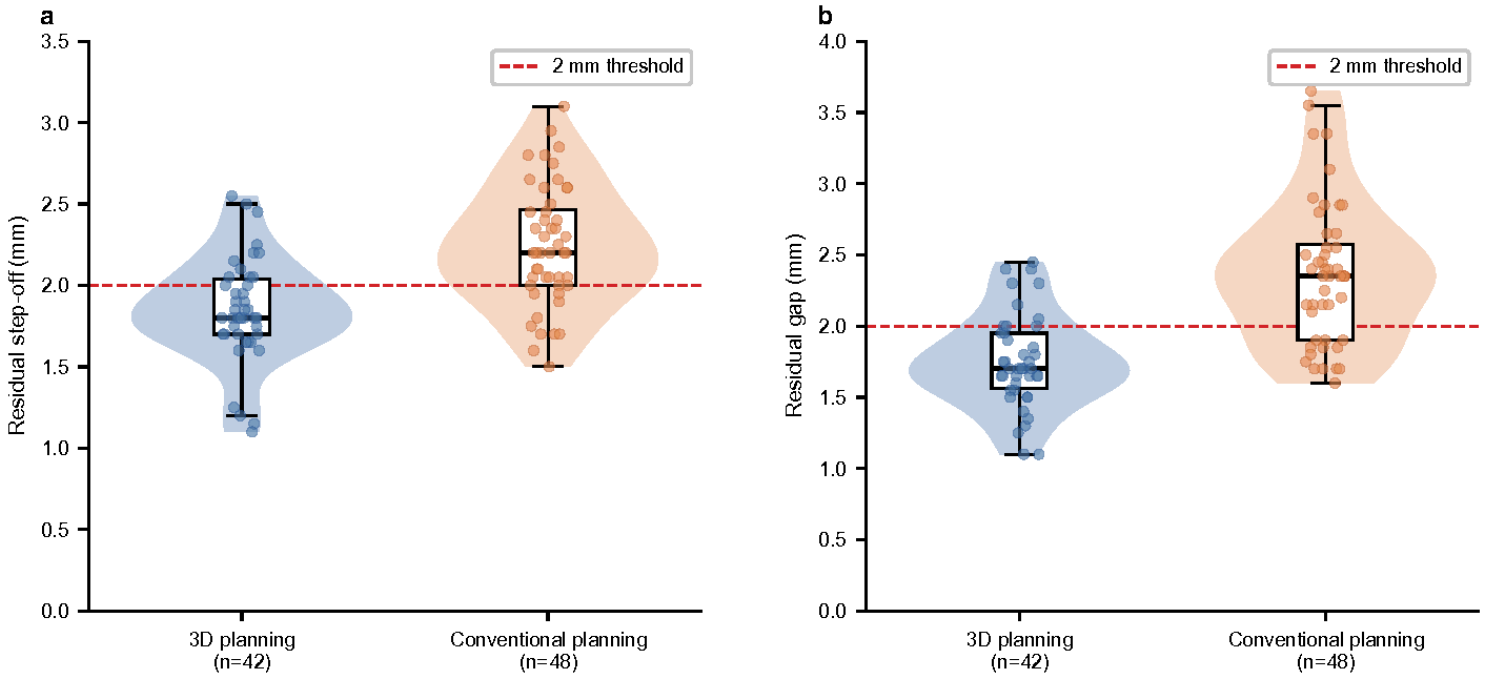


Figure 4

Distribution of early residual displacement. Foot-level distributions of residual posterior-facet step-off (a) and gap (b) are shown for the 3D-planning group (n=42 feet) and conventional-planning group (n=48 feet). Points represent individual feet and are plotted once; violin width represents the kernel-density estimate. Boxes show the median and interquartile range, and whiskers extend to the most extreme values within 1.5 times the interquartile range. Values beyond the whiskers remain represented by their individual filled points; separate boxplot outlier glyphs were suppressed to avoid duplicate display. The dashed line marks the exploratory 2-mm imaging threshold, which is not a validated patient-important cutoff.

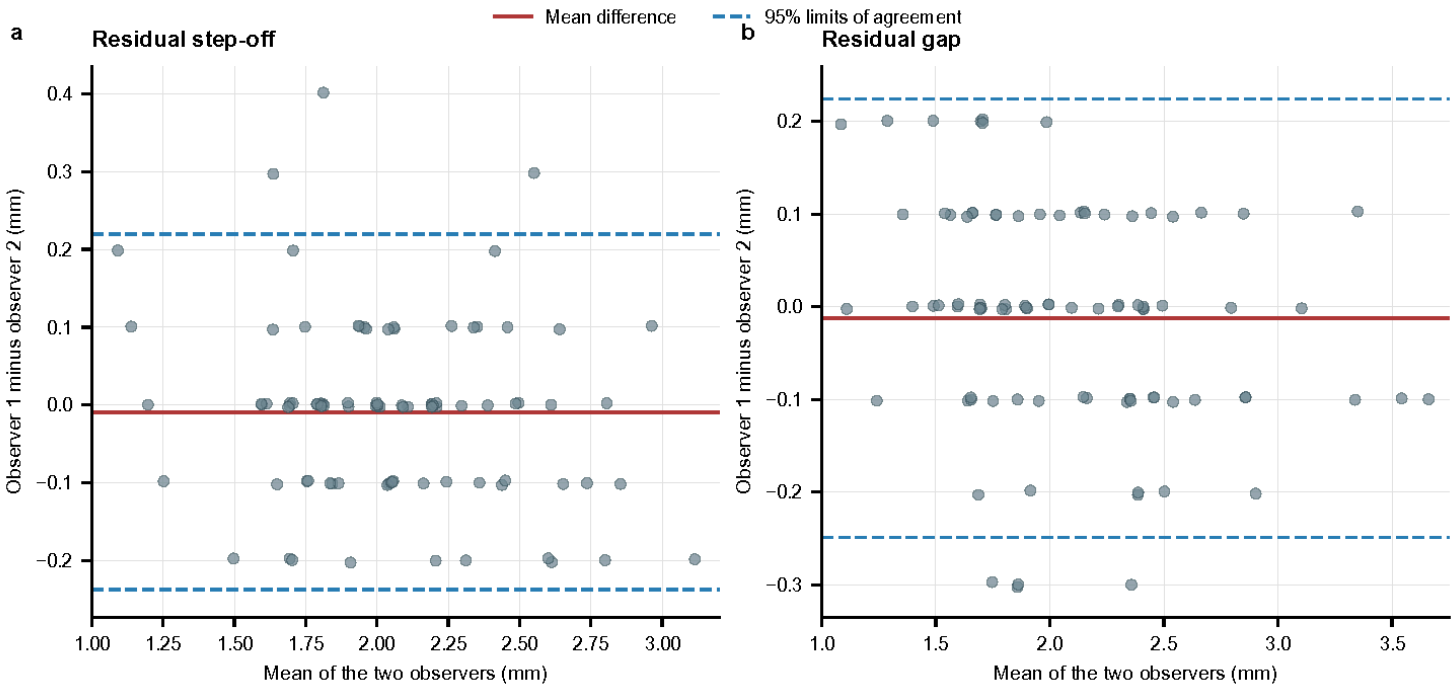


Figure 5

Agreement between CT observers. Bland-Altman plots for residual step-off (a) and gap (b), each based on 90 feet. The x-axis shows the mean of the two observer measurements, and the y-axis shows observer 1 minus observer 2. Small deterministic jitter was added only for display of measurements recorded at 0.1-mm increments and did not alter the analyzed values. Solid red lines show the mean between-observer difference; dashed blue lines show the upper and lower 95% limits of agreement. For step-off, the mean difference was −0.009 mm and the limits were −0.238 to 0.220 mm. For gap, the mean difference was −0.012 mm and the limits were −0.249 to 0.224 mm.

Supplementary Files

This is a list of supplementary files associated with this preprint. Click to download.

- Additionalfile1STROBEchecklist.docx
- Additionalfile2Sensitivityanalyses.xlsx
- Additionalfile3Reproducibleanalysiscode.zip